Chapter 8.6 Advanced Methods

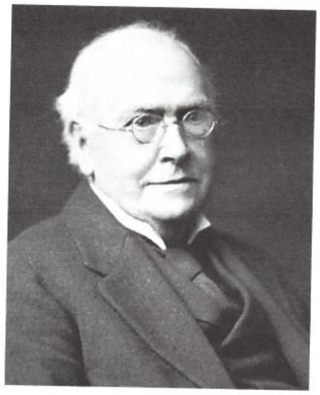

SIR HORACE LAMB

Sir Horace Lamb (1849–1934) is best known for his extremely thorough and well-written book, *Hydrodynamics*, which first appeared in 1879 and has been reprinted numerous times. It still serves as a compendium of useful information as well as the source for a great number of papers and books. If this present book has but a small fraction of the appeal of *Hydrodynamics*, the authors would be well satisfied.

Sir Horace Lamb was born in Stockport, England in 1849, educated at Owens College, Manchester, and then Trinity College, Cambridge University, where he studied with professors such as J. Clerk Maxwell and G. G. Stokes. After his graduation, he lectured at Trinity (1822–1825) and then moved to Adelaide, Australia, to become Professor of Mathematics.

After ten years, he returned to Owens College (part of Victoria University of Manchester) as Professor of Pure Mathematics; he remained until 1920.

Professor Lamb was noted for his excellent teaching and writing abilities. In response to a student tribute on the occasion of his eightieth birthday, he replied: "I did try to make things clear, first to myself . . . and then to my students, and somehow make these dry bones live."

His research areas encompassed tides, waves, and earthquake properties as well as mathematics.

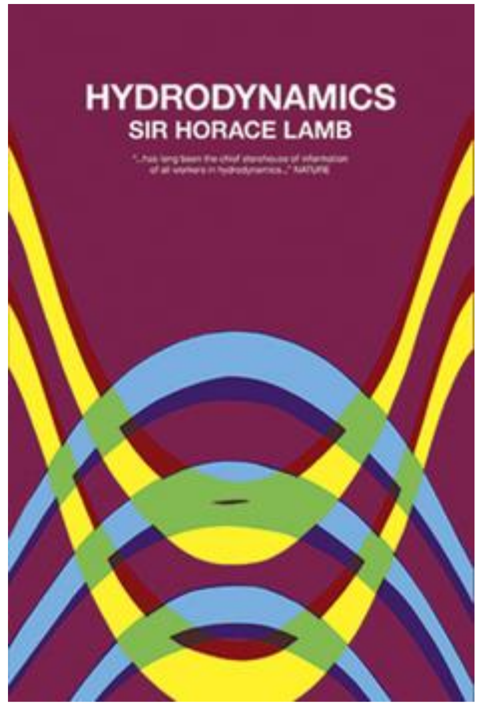

Professor Lamb was noted for his excellent teaching and writing abilities. In response to a student tribute on the occasion of his eightieth birthday, he replied: "I did try to make things clear, first to myself . . . and then to my students, and somehow make these dry bones live."

LOUIS LANDWEBER, professor emeritus of mechanics and hydraulics, Iowa Institute of Hydraulic Research (IIHR)– Hydroscience and Engineering, passed away January 20, 1998, at the age of 86. A distinguished and widely recognized leader and a theoretician whose insights extended well beyond the ordinary, he was the "Father of Ship Hydrodynamics" at IIHR, with a career that spanned decades of the 20th century critical to the development of naval ship hydrodynamics.

Method of Images for Multiple Boundaries:

The method can be extended for multiple boundaries by using successive images.

(1) For example, the solution for a source equally spaced between two parallel planes

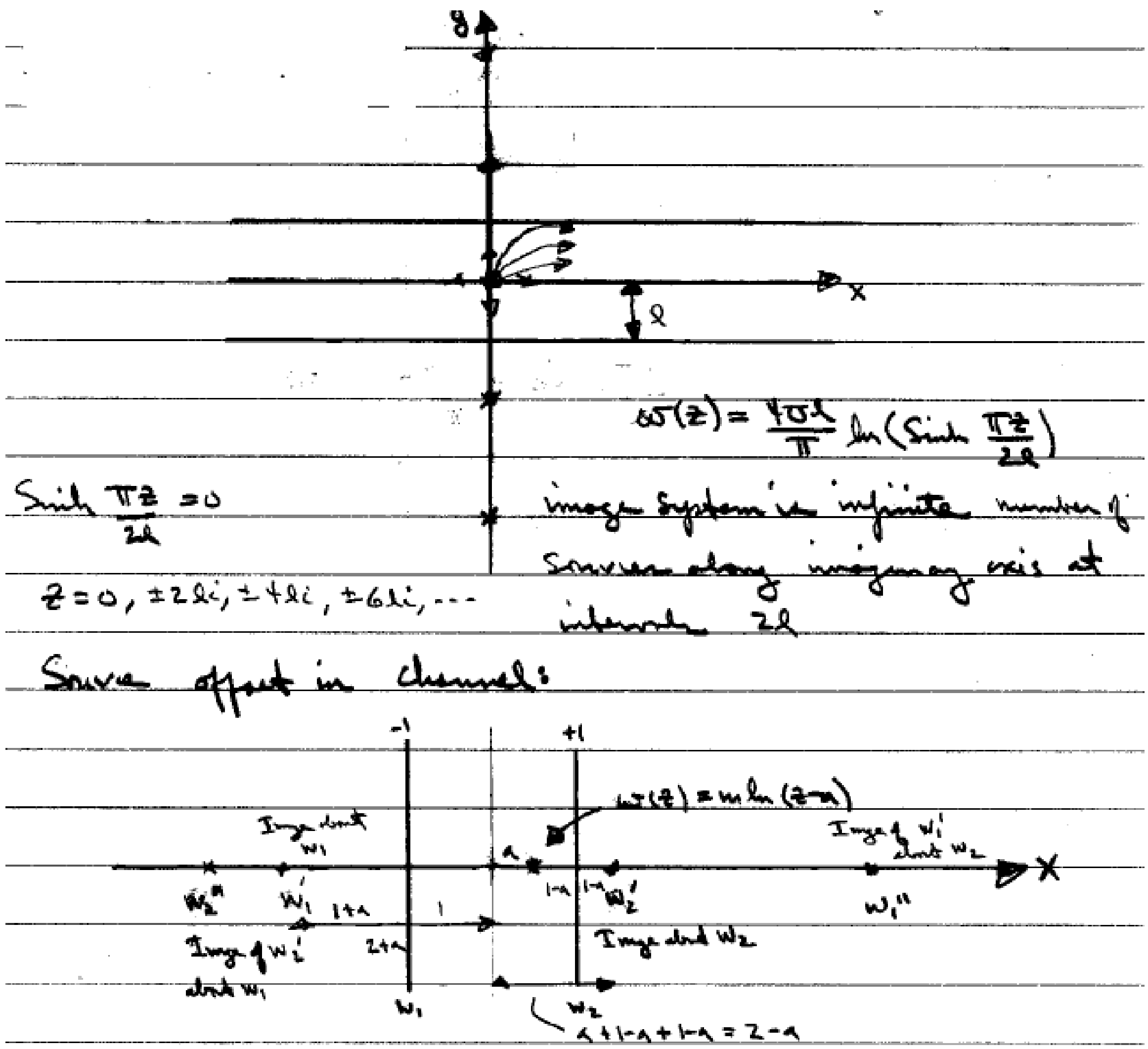

$$w(z) = m \sum_{m=0,\pm1,\pm2,\ldots} \left[\ln\left[z-(4n+a)\right] + \ln\left[z-(4n+2-a)\right] \right]$$

$$= m\left[\ln(z-a) + \ln(z-2+a) + \ln(z-4+a) + \ln(z-6+a) + \ln(z+4-a) + \ln(z+2+a) + \ldots\right]$$

Method of Images Spherical and Curvilinear Boundaries:

The results for plane boundaries are obtained from consideration of symmetry. For spherical and circular boundaries, image systems can be determined from the Sphere & Circle Theorems, respectively. For example:

Flow field	Image System
Source of strength M at c outside sphere of radius a, c>a	Sources of strength ma/c at a^2/c and line sink of strength m/a extending from center of sphere to a^2/c
Dipole of strength μ at l outside sphere of radius a, $l>a$	dipole of strength $-a^3\mu/l$ at $-a^2/l$
Source of strength m at b outside circle of radius a, b>a	equal source at a^2/b and sink of same strength at the center of the circle

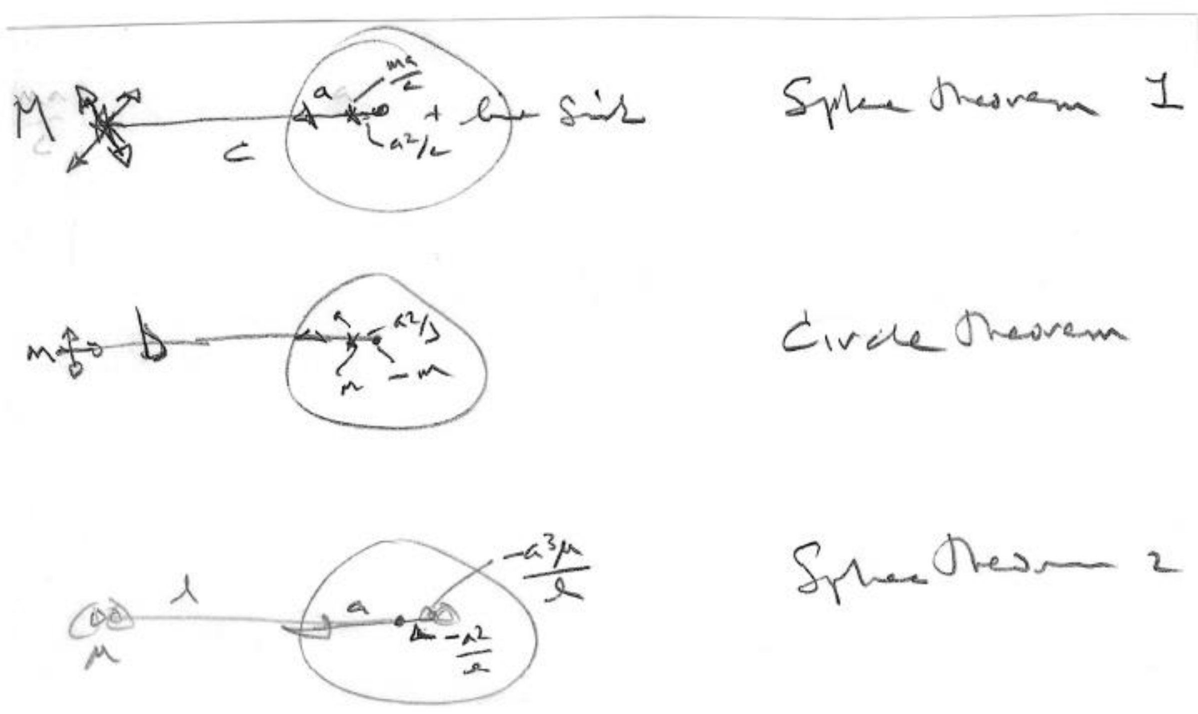

(2) As a second example of the method of successive images for multiple boundaries consider two spheres A and B moving along a line through their centers at velocities U_1 and U_2, respectively:

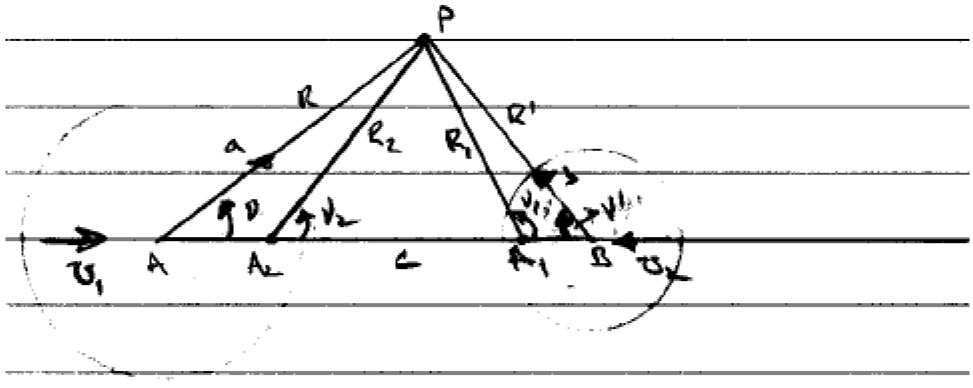

Consider the kinematic BC for A:

$$F(x,t) = (x - yt)^2 + y^2 + z^2 - a^2$$

$$\frac{DF}{Dt} = 0 \Rightarrow \underline{V} \cdot \hat{e}_R = U_1 \hat{k} \cdot \hat{e}_R \text{ or } \phi_R = U_1 \cos\nu$$

where $\varphi = -\frac{\Delta}{R^2}\cos\nu$, $\phi_R = -\frac{2\Delta}{R^3}\cos\nu \Rightarrow \Delta = \frac{Ua^3}{2}$ for single sphere

Similarly for B→ $\phi_R = U_2 \cos\nu'$

This suggests the potential in the form

$$\varphi = U_1\varphi_1 + U_2\varphi_2$$

where ϕ_1 and ϕ_2 both satisfy the Laplace equation and the boundary condition:

$$\left(\frac{\partial \phi_1}{\partial R}\right)_{R=a} = \cos\nu, \quad \left(\frac{\partial \phi_1}{\partial R'}\right)_{R'=b} = 0 \qquad (*)$$

$$\left(\frac{\partial \phi_2}{\partial R}\right)_{R=a} = 0, \quad \left(\frac{\partial \phi_2}{\partial R'}\right)_{R'=b} = \cos\nu' \qquad (**)$$

ϕ_1 = potential when sphere A moves with unit velocity towards B, with B at rest
ϕ_2 = potential when sphere B moves with unit velocity towards A, with A at rest

If B were absent.

$$\phi_1 = -\frac{a^3}{2R^2}\cos\nu = -\frac{\Delta_0}{R^2}\cos\nu\,,\ \Delta_0 = \frac{a^3}{2}$$

but this does not satisfy the second condition in (*). To satisfy this, we introduce the image of Δ_0 in B, which is a doublet Δ_1 directed along BA at A_1, the inverse point of A with respect to B. This image requires an image Δ_2 at A_2, the inverse of A_1 with respect to A, and so on. Thus we have an infinite series of images A_1, A_2, … of strengths $\Delta_1, \Delta_2, \Delta_3$ etc. where the odd suffixes refer to points within B and the even to points within A.

Let $f_n = AA_n$ & $AB = c$

$$f_1 = c - \frac{b^2}{c}\,,\ f_2 = \frac{a^2}{f_1}\,,\ f_3 = c - \frac{b^2}{c - f_2}\,,\ldots$$

$$\Delta_1 = \Delta_0\left(-\frac{b^3}{c^3}\right),\ \Delta_2 = \Delta_1\left(-\frac{a^3}{f_1^{\,3}}\right),\ \Delta_3 = \Delta_2\left(-\frac{b^3}{(c-f_2)^3}\right),\ldots$$

where Δ_1 = image dipole strength, Δ_0 = dipole strength $\times \frac{\text{radius}^3}{\text{sistance}^3}$

$\phi_1 = -\frac{\Delta_0\cos\nu}{R^2} - \frac{\Delta_1\cos\nu_1}{R_1^{\,2}} - \frac{\Delta_2\cos\nu_2}{R_2^{\,2}} - \ldots$ with a similar development procedure for ϕ_2. Although exact, this solution is of unwieldy form. Let's investigate the possibility of an approximate solution which is valid for large c (i.e. large separation distance)

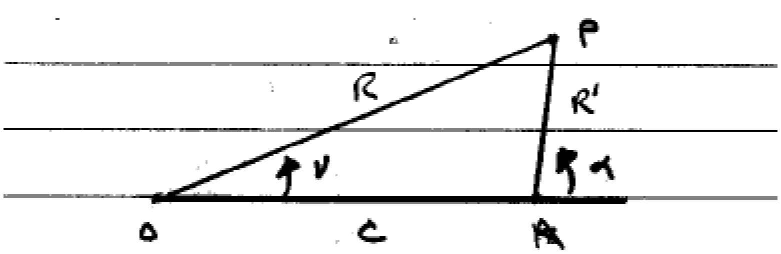

$$R'^2 = R^2 + c^2 - 2cr\cos\nu = R^2\left(1 - \frac{2c}{R}\cos\nu + \frac{c^2}{R^2}\right)$$

$$\frac{1}{R'} = \frac{1}{R}\left[1 - 2\frac{c}{R}\cos\nu + \frac{c^2}{R^2}\right]^{-\frac{1}{2}} = \frac{1}{c}\left[1 - 2\frac{R}{c}\cos\nu + \frac{R^2}{c^2}\right]^{-\frac{1}{2}}$$

Considering the former representation first defining $\mu = \frac{c}{R}$ and $u = \cos\upsilon$

$$\frac{1}{R'}=\frac{1}{R}\left[1-2u\mu+\mu^2\right]^{-\frac{1}{2}}$$

By the binomial theorem valid for $|x|<1$

$$(1-x)^{-\frac{1}{2}}=\alpha_0+\alpha_1 x+\alpha_2 x^2+\alpha_3 x^3+\cdots,\ \alpha_0=1 \text{ and } \alpha_n=\frac{1\cdot 3\cdot(2n-1)}{2\cdot 4\cdot 2n}$$

Hence if $|2u\mu-\mu^2<1|$

$$[\ ]^{-\frac{1}{2}}=\alpha_0+\alpha_1\left(2u\mu-\mu^2\right)+\alpha_2(\ )^2+\cdots=P_0(u)+P_1(u)\mu+P_2(u)\mu^2$$

After collecting terms in powers of μ, where the P_n are Legendre functions of the first kind (i.e. Legendre polynomials which are Legendre functions of the first kind of order zero). Thus,

$$R<C:\frac{1}{R'}=\frac{1}{c}+\frac{R}{c^2}P_1(\cos\nu)+\frac{R^2}{c^3}P_2(\cos\nu)+\cdots$$

$$R>C:\frac{1}{R'}=\frac{1}{R}+\frac{c}{R^2}P_1(\cos\nu)+\frac{c^2}{R^3}P_2(\cos\nu)+\cdots$$

Next, consider a doublet of strength Δ at A

$$\phi=-\frac{\Delta\cos\alpha}{R'^2}=\frac{-\Delta(R\cos\nu-c)}{\left(R^2+c^2-2cR\cos\nu\right)^{\frac{3}{2}}}=-\Delta\frac{\partial}{\partial c}\left[\frac{1}{\left(R^2+c^2-2cR\cos\nu\right)^{\frac{1}{2}}}\right]$$

Thus,

$$R<c:\phi=\frac{-\Delta\cos\alpha}{R'^2}=\Delta\left[\frac{1}{c^2}+\frac{2RP_1(\cos\nu)}{c^3}+\frac{3R^2P_2(\cos\nu)}{c\nu}+\cdots\right]$$

$$R>c:\phi=-\Delta\left[\frac{1}{R^2}P_1(\cos\nu)+\frac{2c}{R^3}P_2(\cos\nu)+\frac{3c^2}{R^4}P_3(\cos\nu)+\cdots\right]$$

Going back to the two sphere problem. If B were absent

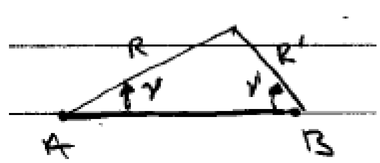

$$\phi_1=-\frac{a^3}{2R^2}\cos\nu$$

using the above expression for the origin at B and near B $\left(\frac{R'}{c}<1\right)$, R→R', $\nu\to\nu'$

$$\phi = -\frac{a^3}{2R^2}\cos\nu = -\left[\frac{1}{2}\frac{a^3}{c^2} + \frac{a^3 R' P_1(\cos\nu)}{c^3} + \cdots\right]$$

$$\phi_R = \frac{-a^3\cos\nu}{c^3} + \cdots$$

which can be cancelled by adding a term to the first approximation, i.e.

$$\phi_1 = -\frac{1}{2}\frac{a^3\cos\nu}{R^2} - \frac{1}{2}\frac{a^3b^3}{c^3}\frac{\cos\nu'}{R'^2}$$

to confirm this

$$\phi_1 = -\frac{1}{2}\frac{a^3}{c^2} - \frac{a3R'\cos\nu'}{c^3} - \frac{1}{2}\frac{a^3b^3}{c^3}\frac{\cos\nu}{R}$$

$$\frac{\partial\phi_1}{\partial R'}(R' = b) = -\frac{a^3\cos\nu'}{c^3} + \frac{a^3b^3}{c^3}\frac{\cos\nu'}{R'^3} = 0 + hot$$

Similarly, the solution for f2 is

$$\phi_2 = -\frac{1}{2}\frac{b^3\cos\nu'}{R'^2} - \frac{1}{2}\frac{a^3b^3}{c^3}\frac{\cos\nu}{R^2}$$

These approximate solutions are converted to $\mathrm{O}\left(c^{-3}\right)$.

To find the kinetic energy of the fluid, we have

$$K = -\frac{1}{2}\rho\left[\int_{S_A}\phi\phi_n dS + \int_{S_B}\phi\phi_n dS\right]$$

$$K = \frac{1}{2}\left[A_{11}U_1^2 + A_{12}U_1U_2 + A_{22}U_2^2\right] = -\frac{\rho}{2}\int_{S_A+S_B}\phi\phi_n dS$$

$$A_{11} = -\rho\int_A \phi_1\frac{\partial\phi_1}{\partial n}dS_A\,,\ A_{22} = -\rho\int_B \phi_2\frac{\partial\phi_2}{\partial n}dS_B\,,\ A_{12} = -\rho\int_A \phi_2\frac{\partial\phi_1}{\partial n}dS_A = -\rho\int_B \phi_1\frac{\partial\phi_1}{\partial n}dS_B$$

where $dS = 2\pi R^2\sin\upsilon d\upsilon$

$A_{11} = \frac{2}{3}\pi a^3\rho\,,\ A_{12} = \frac{2\pi a^3b^3}{c^3}\rho\,,\ A_{22} = \frac{2}{3}\pi b^3\rho\,,$

$K = \frac{1}{4}M'_1U_1^2 + \frac{2\pi a^3b^3\rho}{c^3}U_1U_2 + \frac{1}{4}M'_2U_2^2$: using the approximate form of the potentials

where $\frac{1}{4}M'_1U_1^2, \frac{1}{4}M'_2U_2^2$: masses of liquid displaced by sphere.

Complex variable and conformal mapping

This method provides a very powerful method for solving 2-D flow problems. Although the method can be extended for arbitrary geometries, other techniques are equally useful. Thus, the greatest application is for getting simple flow geometries for which it provides closed form analytic solution which provides basic solutions and can be used to validate numerical methods.

Function of a complex variable

Conformal mapping relies entirely on complex mathematics. Therefore, a brief review is undertaken at this point.

A complex number z is a sum of a real and imaginary part; $z =$ real + i imaginary

The term i, refers to the complex number $i = \sqrt{-1}$

so that; $$i = \sqrt{-1},\quad i^2 = -1,\quad i^3 = -i,\quad i^4 = 1$$

Complex numbers can be presented in a graphical format. If the real portion of a complex number is taken as the abscissa, and the imaginary portion as the ordinate, a two-dimensional plane is formed.

$z = real + i\ imaginary = x + iy$

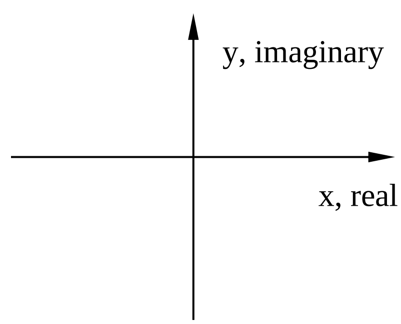

-A complex number can be written in polar form using Euler's equation;

$$z = x + iy = re^{i\theta} = r(\cos\theta + i\cdot\sin\theta)$$

Where: $r^2 = x^2 + y^2$

- Complex multiplication: $z_1 \cdot z_2 = (x_1+iy_1)(x_2+iy_2) = (x_1x_2 - y_1y_2) + i(x_1y_2 + y_1x_2)$

$$= r_1e^{i\theta_1}\cdot r_2e^{i\theta_2} = r_1r_2\cdot e^{i(\theta_1+\theta_2)}$$

- Conjugate: $z = x + iy$ $\quad \bar{z} = x - iy$ $\quad z.\bar{z} = x^2 + y^2$

-Complex function:

$$\boldsymbol{w(z) = f(z) = \phi(x,y) + i\psi(x,y)}$$

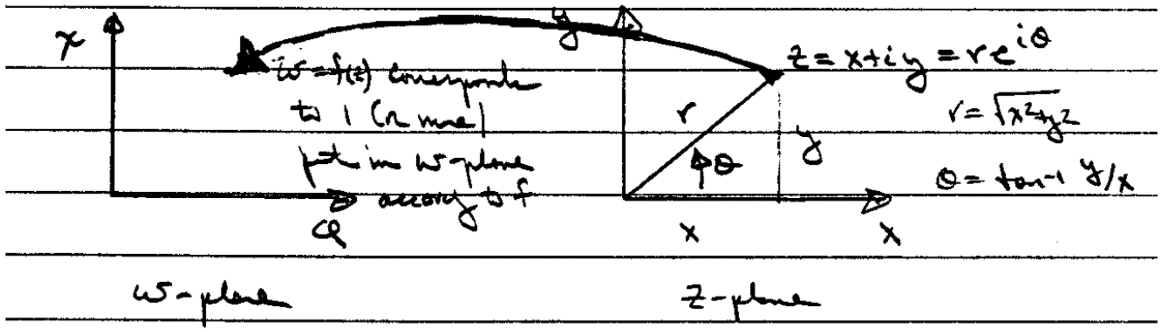

If function w(z) is differentiable for all values of z in a region of z plane is said to be regular and analytic in that region. Since a complex function relates two planes, a point can be approached along an infinite number of paths, and thus, in order to define a unique derivative f(z) must be independent of path.

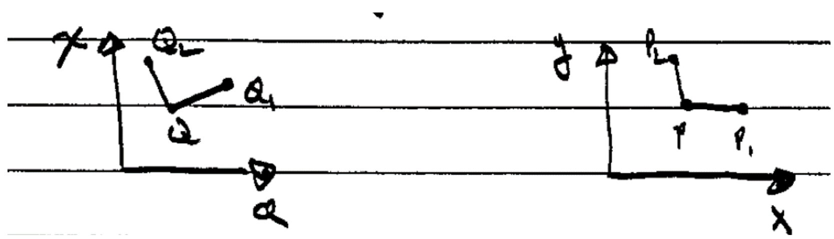

$$PP1(\delta y = 0): \qquad \frac{\delta w}{\delta z} = \frac{w_1 - w}{z_1 - z} = \frac{\phi_1 + i\psi_1 - (\phi + i\psi)}{x_1 - x}$$

$$\Rightarrow \left.\frac{dw}{dz}\right|_1 = \phi_x + i\psi_x$$

$Note: \ w_1 = \phi_1(x + \delta x, y) + i\psi_1(x + \delta x, y)$

$$PP2(\delta x = 0): \qquad \frac{\delta w}{\delta z} = \frac{w_2 - w}{z_2 - z} = \frac{\phi_2 + i\psi_2 - (\phi + i\psi)}{i(y_2 - y)}$$

$$\Rightarrow \left.\frac{dw}{dz}\right|_2 = -i\phi_y + \psi_y$$

For $\frac{dw}{dz}$ to be unique and independent of path:

$\phi_x = \psi_y \ and -\phi_y = \psi_x$ Cauchy Riemann Eq.

Recall that the velocity potential and stream function were shown to satisfy this relationship as a result of their othogonality. Thus, complex function $w = \phi + i\psi$ represents 2-D flows. $\phi_{xx} = \psi_{yx}$ $\phi_{yy} = -\psi_{xy}$ i.e. $\phi_{xx} + \phi_{yy} = 0$ and similarly, for ψ. Therefore if analytic and regular also harmonic, i.e., satisfy Laplace equation.

Application to potential flow

$w(z) = \phi + i\psi$ Complex potential where ϕ : velocity potential, ψ : stream function

$$\frac{dw}{dz} = \phi_x + i\psi_x = u - iv = \left(u_r - iu_\theta\right)e^{-i\theta}$$ Complex velocity

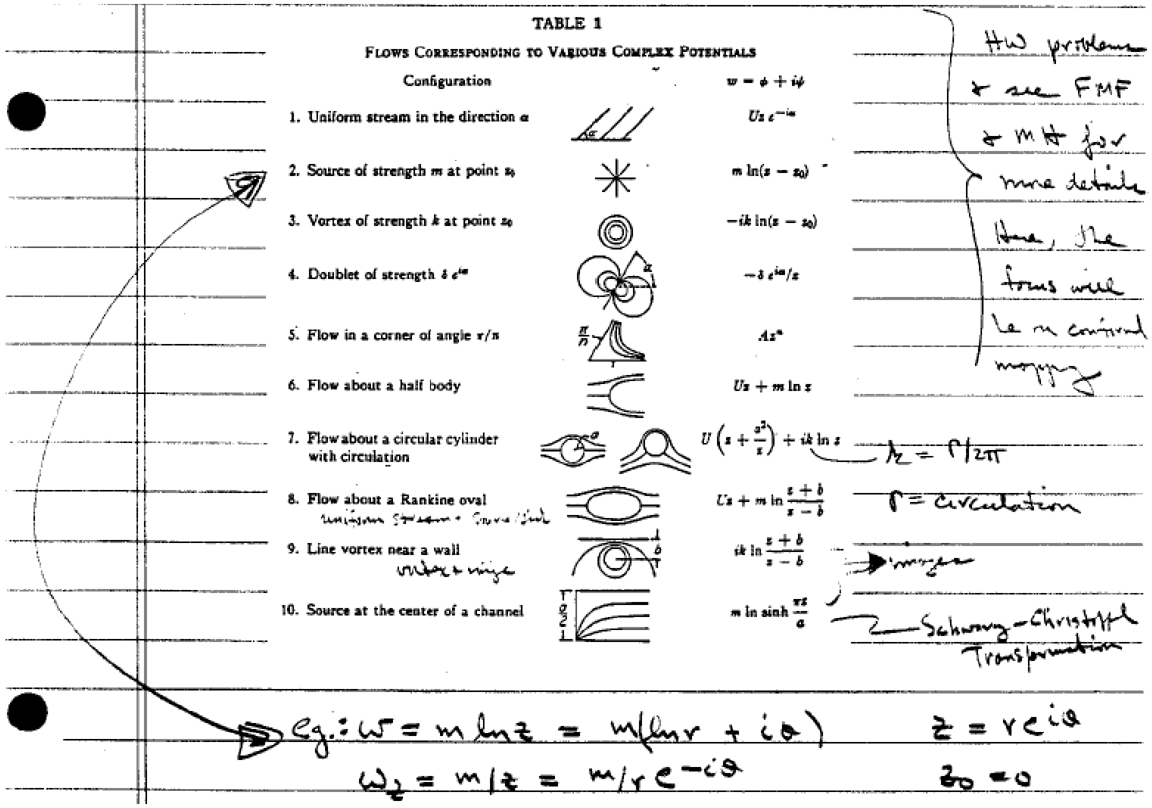

TABLE 1

FLOWS CORRESPONDING TO VARIOUS COMPLEX POTENTIALS

Configuration	$w = \phi + i\psi$
1. Uniform stream in the direction α	$Uz\,e^{-i\alpha}$
2. Source of strength m at point z_0	$m \ln(z - z_0)$
3. Vortex of strength k at point z_0	$-ik \ln(z - z_0)$
4. Doublet of strength $\delta\,e^{i\alpha}$	$-\delta\,e^{i\alpha}/z$
5. Flow in a corner of angle π/n	Az^n
6. Flow about a half body	$Uz + m \ln z$
7. Flow about a circular cylinder with circulation	$U\left(z + \frac{a^2}{z}\right) + ik \ln z$
8. Flow about a Rankine oval	$Uz + m \ln \frac{z+b}{z-b}$
9. Line vortex near a wall	$ik \ln \frac{z+b}{z-b}$
10. Source at the center of a channel	$m \ln \sinh \frac{\pi z}{a}$

$r'e^{i\theta'} = \rho r e^{i(\theta+\alpha)}$ where $r' = \rho r$ (magnification) and $\theta' = \theta + \alpha$ (rotation)

→Triangle about z_0 is transformed into a similar triangle in the ζ-plane which is magnified and rotated.

Implication:

-Angles are preserved between the intersections of any two lines in the physical domain and in the mapped domain.

-The mapping is one-to-one, so that to each point in the physical domain, there is one and only one corresponding point in the mapped domain.

For these reasons, such transformations are called conformal.

Usually the flow-field solution in the ζ-plane is known:

$$W(\varsigma) = \Phi(\xi,\eta) + i\Psi(\xi,\eta)$$

Then

$$w(z) = W\big(f(z)\big) = \phi(x,y) + i\psi(x,y) \text{ or } \phi = \Phi \;\&\; \psi = \Psi$$

Conformal mapping

The real power of the use of complex variables for flow analysis is through the application of conformal mapping: techniques whereby a complicated geometry in the physical z-domain is mapped onto a simple geometry in the ζ-plane (circular cylinder) for which the flow-field solution is known. The flow-field solution in the z-plane is obtained by relating the ζ-plane solution to the z-plane through the conformal transformation ζ=f(z) (or inverse mapping z=g(ζ)).

Before considering the application of the technique, we shall review some of the more important properties and theorems associated with it.

Consider the transformation,
ζ=f(z) where f(z) is analytic at a regular point Z_0 where $f'(z_0) \neq 0$
$\delta\zeta = f'(z_0)\,\delta z$
$\delta\varsigma = r' e^{i\theta'}, \delta z = re^{i\theta}, f'(z_0) = \rho e^{i\alpha}$

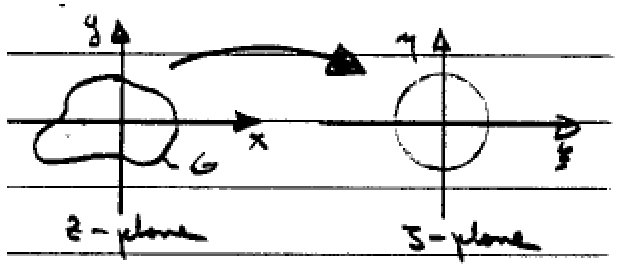

→The streamlines and equipotential lines of the ζ-plane (Φ, Ψ) become the streamlines of equipotential lines of the z-plane (ϕ, ψ).

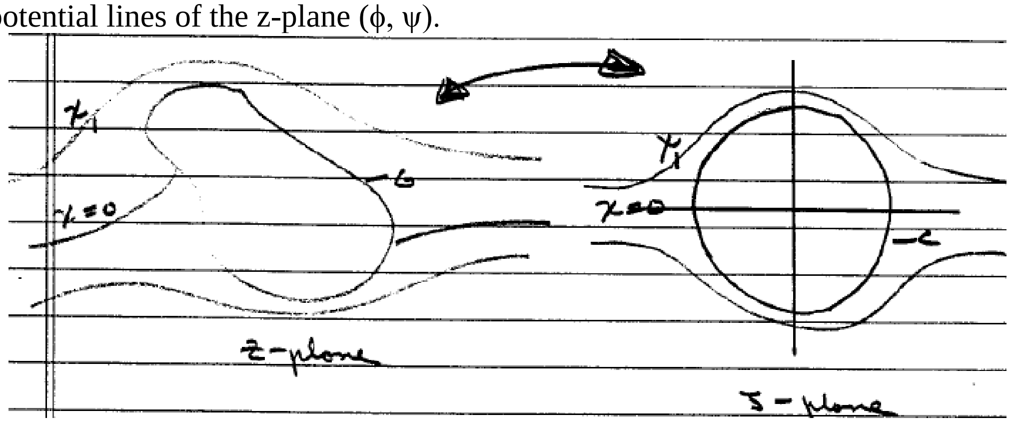

$\rightarrow \begin{matrix} \nabla_z^2\varphi = \nabla_\varsigma^2\phi = 0 \\ \nabla_z^2\psi = \nabla_\varsigma^2\psi = 0 \end{matrix}$ i.e. Laplace equation in the z-plane transforms into Laplace equation is the ζ-plane.

The complex velocities in each plane are also simply related

$$\frac{dw}{dz} = \frac{dw}{d\varsigma}\frac{d\varsigma}{dz} = \frac{dw}{d\varsigma} f^{'}(z)$$

$$\frac{dw}{dz}(z) = u - iv = (U - iV) f'(z) = \frac{dW}{d\zeta}(\zeta = f(z))$$

i.e. velocities in two planes are proportional.

Two independent theorems concerning conformal transformations are:

(1) Closed curves map to closed curves
(2) Rieman mapping theorem: an arbitrary closed profile can be mapped onto the unit circle.

More theorems are given and discussed in AMF Section 43. Note that these are for the interior problems, but are equally valid for the exterior problems through the inversion mapping.

Many transformations have been investigated and are compiled in handbooks. The AMF contains many examples:

1) Elementary transformations:

a) linear: $w = \dfrac{az+b}{cz+d}, ad - bc \neq 0$

b) corner flow: $w = Az^n$

c) Jowkowsky: $w = \varsigma + c^2/\varsigma$

d) exponential: $w = e^n$

e) $w = z^s$, s irational

2) Flow field for specific geometries

a) circle theorem
b) flat plate
c) circular arc
d) ellipse
e) Jowkowski foils
f) ogive (two circular areas)
g) Thin foil theory [solutions by mapping flat plate with thin foil BC onto unit circle]
h) multiple bodies

3) Schwarz-Cristoffel mapping

4) Free-streamline theory

The techniques of conformal mapping are best learned through their applications. Here we shall consider corner flow.

A simple example: Corner flow

1. In ζ-plane, let $W(\varsigma) = \varsigma$ i.e. uniform stream

2. Say→ $\varsigma = f(z) = z^{\pi/\theta}$

3. $w(z) = W(f(z)) = z^{\pi/\theta}$ i.e. corner flow

Note that 1-3 are unit uniform stream.

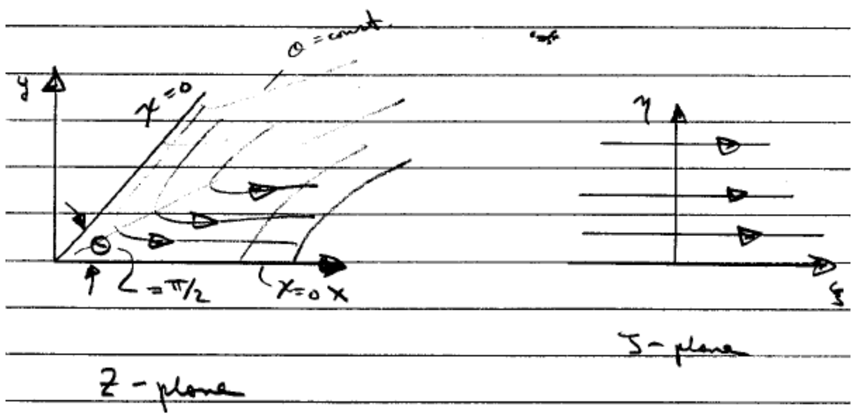

$$w(z) = Uz^n = UR^n \cos\theta + iUR^n \sin n\theta \text{, where } z = \mathrm{R}e^{i\theta}$$

i.e. $\phi = UR^n \cos n\theta$, $\psi = UR^n \sin n\theta$

$\psi = UR^n \sin n\theta$ =const.=streamlines

$\phi = UR^n \cos n\theta$ =const.=equipotentials

$$\frac{dw}{dz} = \frac{dW}{d\varsigma}\frac{d\varsigma}{dz} = nUz^{n-1} = nUR^{n-1}e^{i(n-1)\theta} = (nUR^{n-1}\cos n\theta + inUR^{n-1}\sin n\theta)e^{-i\theta}$$

$$= (u_r - iu_\theta)e^{-i\theta}$$

$$u_r = nUR^{n-1}\cos n\theta$$

$$u_\theta = -nUR^{n-1}\sin n\theta$$

$$0 < \theta < \left(\pi/2n\right) \rightarrow u_r > 0,\ u_\theta < 0$$

$$\left(\pi/2n\right) < \theta < \left(\pi/n\right) \rightarrow u_r < 0,\ u_\theta < 0$$

i.e. $w(z) = Uz^n$

represents corner flow: n=1→uniform stream, n=2→90° corner

Introduction to Surface Singularity methods (also known as Boundary Integral and Panels Methods)

Next, we consider the solution of the potential flow problem for an arbitrary geometry. Consider the BVP for a body of arbitrary geometry fixed in a uniform stream of an inviscid, incompressible, and irrotational fluid.

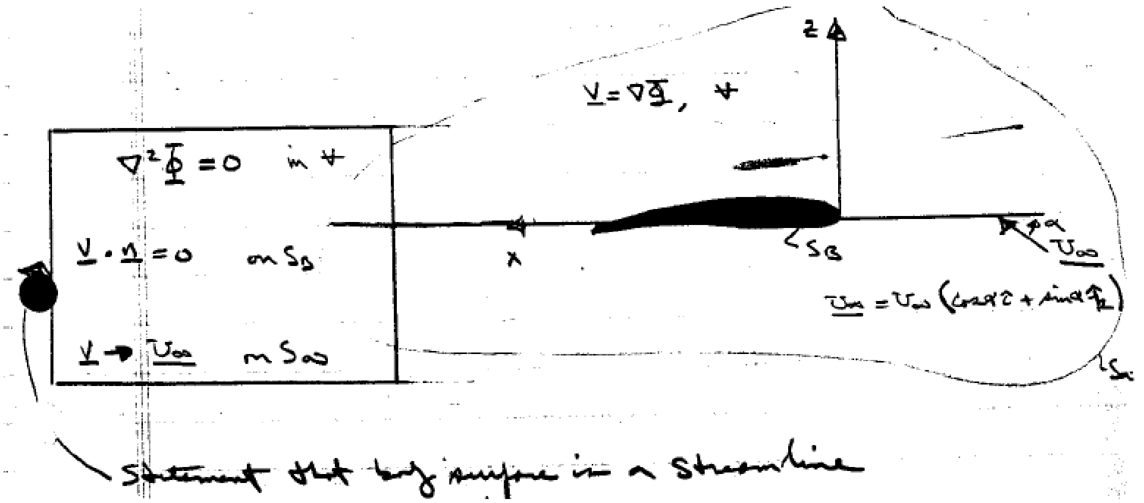

The surface singularity method is founded on the symmetric form of Greens theorem and what is known as Greens function.

$$\int_V \left(G\nabla^2\Phi - \Phi\nabla^2 G\right) dV = \int_{\sum S=S_\infty+S_B+S_S} \left(G\frac{\partial\Phi}{\partial n} - \Phi\frac{\partial G}{\partial n}\right) dS \qquad (1)$$

where Φ and G are any two scalar field in V (control volume bounded by s infinity S body and S inserted to render the domain simply connected) and for our application.
Φ= velocity potential
G= Green's function

Say,
$\nabla^2 G = -\delta(\underline{x} - \underline{x_0})$ in V+V' (i.e. entire domain) where δ is the Dirac delta function.
G→0 on S_∞

Solution for G (obtained Fourier Transforms) is: $G = \ln|\underline{r}|$, $|r| = |\underline{x} - \underline{x_0}|$, i.e. elementary 2-D source at $\underline{x} = \underline{x_0}$ of unit strength, and (1) becomes

$$\Phi = \int_{\sum S=S_B} \left(G\frac{\partial\Phi}{\partial n} - \Phi\frac{\partial G}{\partial n}\right) dS$$

First term in integrand represents source distribution and second term dipole distribution, which can be transformed to vortex distribution using integration by parts. By extending the definition of Φ into V' it can be shown that Φ can be represented by distributions of sources, dipoles or vortices, i.e.

$$\Phi = \int_{\sum S=S_B} \sigma G dS \text{ : source distribution, } \sigma \text{ : source strength}$$

or

$$\Phi = \int_{\sum S=S_B} \lambda \frac{\partial G}{\partial n} dS \text{ : dipole distribution, } \lambda \text{ : dipole strength}$$

Also, it can be shown that a source distribution representation can only be used to represent the flow for a non-lifting body; that is, for lifting flow dipole or vortex distributions must be used.

As this stage, let's consider the solution of the flow about a non-lifting body of arbitrary geometry fixed in a uniform stream. Note that since G→0 on S∞ Φ already satisfy the condition S∞. The remaining condition, i.e. the condition is a stream surface is used to determine the source distribution strength.

Consider a source distribution method for representing non-lifting flow around a body of arbitrary geometry.

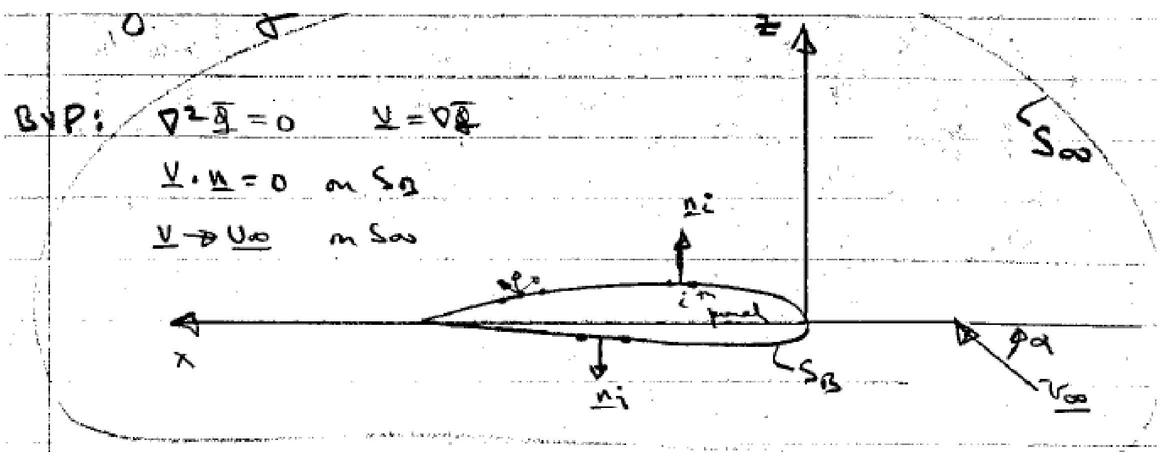

$\underline{V} = \underline{U}_\infty + \nabla\phi$: total velocity

U_∞ : uniform stream, $\nabla\phi$: perturbation potential due to presence of body

$\underline{U}_\infty = U_\infty(\cos\alpha\hat{i} + \sin\alpha\hat{j})$: note that for non-lifting flow Γ must be zero (i.e. for a symmetric foil $\alpha = 0$ or for cambered filed $\alpha = \alpha_{oLift}$)

$$\phi = \int_{S_B} \frac{K}{2\pi} \ln r ds \text{ : source distribution on body surface}$$

Now, K is determined from the body boundary condition.

$\underline{V}\cdot\underline{n}=0$ i.e. $\underline{U}_\infty\cdot\underline{n}+\nabla\phi\cdot\underline{n}=0$ or $\frac{\partial\phi}{\partial n}=-\underline{U}_\infty\cdot\underline{n}$

i.e. normal velocity induced by sources must cancel uniform stream→

$$\frac{\partial}{\partial n}\int_{S_B}\frac{K}{2\pi}\ln r ds=-\underline{U}_\infty\cdot\underline{n}$$

This singular integral equation for K is solved by descretizing the surface into a number of panels over which K is assumed constant, i.e. we write

$$\frac{\partial}{\partial n_i}\sum_{j=1}^{M=\text{no. of panels}}\frac{Kj}{2\pi}\int_{Si}\ln r_{ij}dS_i=-\underline{U}_\infty\cdot\underline{n}_i\text{ , i=1,M, j=1,M}$$

where $r_{ij}=\sqrt{(x_i-x_j)^2+(z_i-z_j)^2}$ =distance from ith panel control point to $\underline{r_j}=$position vector along jth panel.

Note that the integral equation is singular since

$$\frac{\partial}{\partial n_i}\ln r_{ij}=\frac{1}{r_{ij}}\frac{\partial r_{ij}}{\partial n_i}$$

at for $r_{ij}=0$ this integral blows up; that is, when i=j and we trying to determine the contribution of the panel to its own source strength. Special care must be taken. It can be shown that the limit does exist at the integral equation can be written

$$\frac{K_i}{2\pi}\frac{\partial}{\partial n_i}\int_{S_j\to S_i}\ln r_{ij}dS_i=\frac{K_i}{2}$$

$$\frac{K_i}{2}+\sum_{\substack{i=1\\j\neq i}}^{M}\frac{K_j}{2\pi}\int_{S_i}\frac{1}{r_{ij}}\frac{\partial r_{ij}}{\partial n_{ij}}dS_j=-\underline{U}_\infty\cdot\underline{n_i}$$

where $\frac{1}{r_{ij}}\frac{\partial r_{ij}}{\partial n_i}=\frac{1}{r_{ij}}\nabla_i r_{ij}\cdot\underline{n_i}=\frac{1}{r_{ij}}\left[\frac{\partial r_{ij}}{\partial x_i}n_{xi}+\frac{\partial r_{ij}}{\partial z_i}n_{zi}\right]=\frac{1}{r_{ij}^{\ 2}}\left[(x_i-x_j)n_{xi}+(z_i-z_j)n_{zi}\right]$

where $r_{ij}^2=(x_i-x_j)^2+(z_i-z_j)^2$

Consider the i[th] panel

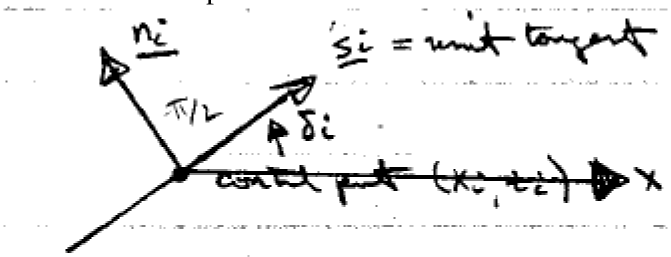

$$\underline{S_i} = \cos\delta_i \hat{i} + \sin\delta_i \hat{j}\,,\ \underline{n_i} = \underline{S_i} \times \hat{j} = -\sin\delta_i \hat{i} + \cos\delta_i \hat{j}$$

$$n_{xi} = -\sin\delta_i\,, n_{zi} = \cos\delta_i$$

$$\frac{\partial}{\partial n}\int_{S_B} \frac{K}{2\pi}\ln r ds = -\underline{U_\infty}\cdot\underline{n}$$

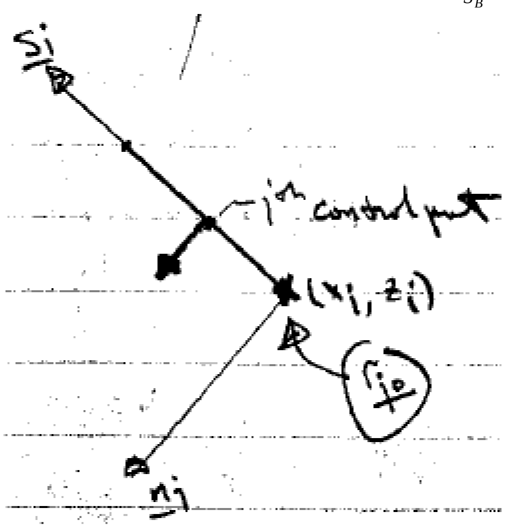

$\underline{r_j} = \underline{r_{j0}} + S\underline{S_i}$, $\underline{r_{j0}}$:origin of j[th] panel coordinate system, $S\underline{S_i}$: distance along j[th] panel

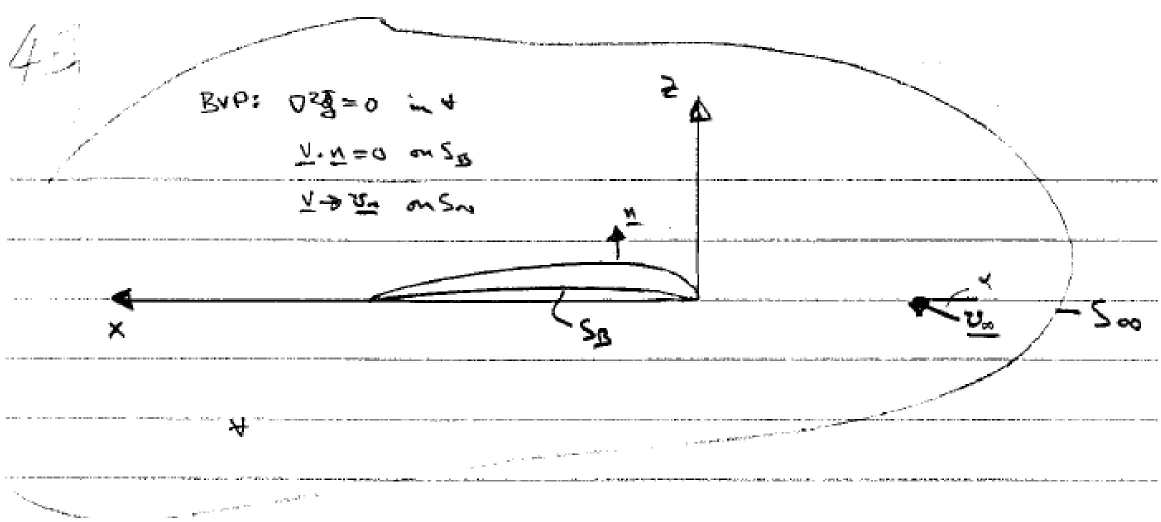

$$\underline{V} = U_\infty + \nabla\phi$$

$$\phi = \int_{S_B} \frac{K}{2\pi} \ln r ds$$

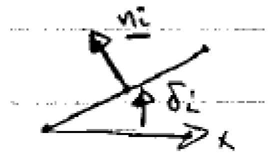

$$\underline{V}\cdot\underline{n} = 0 \rightarrow \frac{\partial}{\partial n}\int_{S_B}\frac{K}{2\pi}\ln r ds = -\underline{U_\infty}\cdot\underline{n}$$

$$\frac{K_i}{2} + \sum_{\substack{i=1\\ j\neq i}}^{M}\frac{K_j}{2\pi}\int_{S_i}\frac{1}{r_{ij}}\frac{\partial r_{ij}}{\partial n_{ij}}dS_j = -\underline{U_\infty}\cdot\underline{n_i} = -U_\infty\sin(\alpha-\delta_i),\ \underline{n_i} = -\sin\delta_i\hat{i} + \cos\delta_i\hat{j}$$

Let $\int_{S_i}\frac{1}{r_{ij}}\frac{\partial r_{ij}}{\partial n_{ij}}dS_j = I_j$ and $RHS_i = -U_\infty\sin(\alpha-\delta_i)$, then

$$\frac{K_i}{2} + \sum_{\substack{i=1\\ j\neq i}}^{M}\frac{K_j}{2\pi}I_j = RHS_i,\ I_j = \int_{S_j}\frac{(x_i-x_j)n_{xi} + (z_i-z_j)n_{zi}}{(x_i-x_j)^2+(z_i-z_j)^2}dS_j$$

$$I_i = \int_0^{l_i}\frac{(x_i-x_{j0}-S_jn_{zj})n_{xi} + (z_i-z_{j0}-S_jn_{xj})n_{zi}}{(x_i-x_{j0}-S_jn_{zj})^2 + (z_i-z_{j0}-S_jn_{xj})^2}dS_j$$

$$= \int_0^{l_i}\frac{(x_i-x_{j0})n_{xi} + (z_i-z_{j0})n_{zi} + S_j(n_{xj}n_{zi}-n_{zj}n_{xi})}{(x_i-x_{j0})^2 + (z_i-z_{j0})^2 + 2S_j[-n_{zi}(x_i-x_{j0}) + n_{zj}(z_i-z_{j0})] + S_j^2}dS_j$$

$$= \int_0^{l_i}\frac{CS_j + D}{S_j^2 + 2AS_j + B}dS_j$$

where

$$A = -\cos\delta_j(x_i-x_{j0}) - \sin\delta_j(z_i-z_{j0})$$

$$B = (x_i-x_{j0})^2 + (z_i-z_{j0})^2$$

$$C = \sin(\delta_i-\delta_j)$$

$$D = -(x_i-x_{j0})\sin\delta_i + (z_i-z_{j0})\cos\delta_i$$

$I_j = D\int_0^{l_i}\frac{1}{X}dS_j + C\int_0^{l_i}\frac{S_i}{X}dS_j = DI_{i1} + CI_{i2}$ where $X = S_j^2 + 2AS_j + B$

I_{j1} depends on if q<0 or >0 where $q = 4B - 4A^2$

$$I_{j2} = \frac{1}{2}\ln X - AI_{i1}$$

$$\frac{K_i}{2} + \sum_{\substack{i=1\\ j\neq i}}^{M}\frac{K_j}{2\pi}\int_{S_j}\frac{(x_i-x_j)n_{xi} + (z_i-z_j)n_{zi}}{(x_i-x_j)^2+(z_i-z_j)^2}dS_j = -\underline{U_\infty}\cdot\underline{n_i} = RHS_i$$

$$RHS_i = -U_\infty[-\cos\alpha\sin\delta_i + \sin\alpha\cos\delta_i] = -U_\infty\sin(\alpha-\delta_i)$$

$\frac{K_i}{2} + \sum_{\substack{i=1 \\ j\neq i}}^{M} \frac{K_j}{2\pi} I_i = RHS_i$: Matrix equation for K_i and can be solved using Standard methods such as Gauss-Siedel Iteration.

In order to evaluate Ij, we make the substitution

$$\begin{aligned} x_j &= x_{j0} + S_j S_{xj} \\ z_j &= z_{j0} + S_j S_{xj} \end{aligned} \rightarrow \underline{r_j} = \underline{r_{j0}} + S_j S_j$$

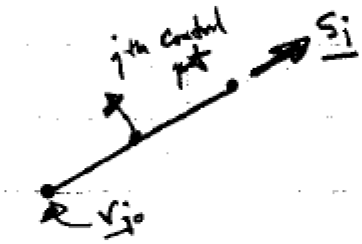

where Sj= distance along the j^th panel $0 \le S_j \le l_i$

$$S_{xj} = n_{zi} = \cos\delta_j$$
$$S_{zj} = n_{xi} = \sin\delta_j$$

After substitution, Ij becomes

$$B - A^2 = (x_i - x_{j0})^2 + (z_i - z_{j0})^2$$
$$-\left[\cos^2\delta_j (x_i - x_{j0})^2 + \sin^2\delta_j (z_i - z_{j0})^2 + 2\cos\delta_j \sin\delta_j (x_i - x_{j0})(z_i - z_{j0})\right]$$
$$= (x_i - x_{j0})^2 (1 - \cos^2\delta_j) + (z_i - z_{j0})^2 (1 - \sin^2\delta_j) - 2$$

$$q = 4(B - A^2) = 4\left[(x_i - x_{j0})\sin\delta_i - (z_i - z_{j0})\cos\delta_i\right]^2$$

i.e. q>0 and as a result,

$$I_{j1} = \frac{2}{\sqrt{q}} \tan^{-1} \frac{2S_i + 2A}{\sqrt{q}} = \frac{1}{E} \tan^{-1} \frac{S_i + A}{E} \text{ where } \sqrt{q} = 2\sqrt{B - A^2} = 2E$$

$$I_j = DI_{j1} + C\left[\frac{1}{2} \ln \mathrm{X} - AI_{j1}\right] = (D - CA) I_{j1} + \frac{C}{2} \ln \mathrm{X}\Big|_0^{l_i}$$
$$= \frac{(D - CA)}{E}\left\{\tan^{-1}\frac{l_i + A}{E} - \tan^{-1}\frac{A}{E}\right\} + \frac{C}{2}\ln\left\{\frac{l_j z + 2Al_j + B}{B}\right\}$$

where $\mathrm{X} = S_i^2 + 2AS_j + B$

Therefore, we can write the integral equation in the form

$$\frac{K_i}{2} + \sum_{\substack{i=1 \\ j\neq i}}^{M} \frac{K_j}{2\pi} I_j = -U_\infty \sin(\alpha - \delta_i)$$

$$\begin{bmatrix} \frac{1}{2} & & \frac{k_j}{2\pi} I_j \\ & \ddots & \\ \frac{k_j}{2\pi} I_j & & \frac{1}{2} \end{bmatrix} \begin{bmatrix} \\ K_i \\ \\ \end{bmatrix} = \begin{bmatrix} \\ RHS_i \\ \\ \end{bmatrix}$$

which can be solved by standard techniques for linear systems of equations with Gauss-Siedel Iteration.

Once Ki is known,

$$\underline{V} = U_\infty + \nabla\phi$$

And p is obtained from Bernoulli equation, i.e.

$$p = 1 - \frac{\underline{V} \cdot \underline{V}}{U_\infty^2}$$

Mentioned potential flow solution only depend on is independent of flow condition, i.e. U∞, i.e. only is scaled

On the surface of the body Vn=0 so that

$C_p = 1 - \frac{V_S^2}{U_\infty^2}$ where $V_S = \underline{V} \cdot \underline{S}$ =tangential surface velocity

$$V_S = \nabla\Phi \cdot \underline{S} = \underline{U_\infty} \cdot \underline{S} + \nabla\varphi \cdot \underline{S}$$

$$V_{S_i} = \underline{U_\infty} \cdot \underline{S_i} + \frac{\partial\varphi}{\partial S} = U_\infty \cos(\alpha - \delta_i) + Q_S$$

where $\underline{U_\infty} \cdot \underline{S_i} = U_\infty \left(\cos\alpha\hat{i} + \sin\alpha\hat{j}\right) \cdot \left(\cos\delta_i\hat{i} + \sin\delta_i\hat{j}\right)$

$$\phi_S = \frac{\partial\phi}{\partial S} = \frac{\partial}{\partial S} \int_{S_B} \frac{K}{2\pi} \ln r ds$$

$\phi_{S_i} = \sum_{\substack{j=1 \\ j \neq i}}^{M} \frac{K_j}{2\pi} \int_{l_j} \frac{\partial}{\partial S_i} \left(\ln r_{ji}\right) dS_j$: j=i term is zero since source panel induces no tangential flow on itself. ($\int_{l_j} \frac{\partial}{\partial S_i} \left(\ln r_{ji}\right) dS_j = J_j$)

$$\frac{\partial}{\partial S_i}\left(\ln r_{ij}\right) = \frac{1}{r_{ij}} \frac{\partial r_{ij}}{\partial S} = \frac{1}{r_{ij}} \nabla_i r_{ij} \cdot \underline{S_i}$$

$$= \frac{1}{r_{ij}} \left[\frac{\partial r_{ij}}{\partial x_i} S_{x_i} + \frac{\partial r_{ij}}{\partial z_i} S_{z_i} \right] = \frac{1}{r_{ij}^{\ 2}} \left\{ \left(x_i - x_j\right) S_{x_i} + \left(z_i - z_j\right) S_{z_i} \right\}$$

where $S_{x_i} = \cos\delta_i, S_{z_i} = \sin\delta_i$

$$C_{p_i} = 1 - \left(\frac{V_{S_i}}{U_\infty}\right)^2, V = -U_\infty \cos(\alpha - \delta_i) + \sum_{\substack{j=1 \\ i \neq j}} \frac{K_i}{2\pi} J_j$$

$$J_{ij} = \int_{l_i} \frac{1}{r_{ij}} \frac{\partial r_{ij}}{\partial S} dS_j = \int_{S_j} \frac{(x_i - x_j)n_{xi} + (z_i - z_j)n_{zi}}{(x_i - x_j)^2 + (z_i - z_j)^2} dS_j$$

$$= \int_0^{l_i} \frac{(x_i - x_{j0} - S_j S_{xj})S_{xi} + (z_i - z_{j0} - S_j S_{zxj})S_{zi}}{(x_i - x_{j0} - S_j S_{xj})^2 + (z_i - z_{j0} - S_j S_{zj})^2} dS_j$$

where $S_{x_i} = \cos\delta_i, S_{z_i} = \sin\delta_i$, $(x_i - x_{j0} - S_j S_{xj})^2 + (z_i - z_{j0} - S_j S_{zj})^2 = S_j^2 + 2AS_j + B$

$$(x_i - x_j)\cos\delta_i + (z_i - z_{i0})\sin\delta_i + S_j(-S_{xj}S_{xi} - S_{zj}S_{zi}) - \cos\delta_j \cos\delta_i - \sin\delta_j \sin\delta_i$$

$$= \int_0^{\lambda_i} \frac{CS_j + D}{S_j^2 - AS_j - C} dS_i$$

$$D = (x_i - x_{j0})\cos\delta_i + (z_i - z_{j0})\sin\delta_i$$

$$C = -\cos(\delta_i - \delta_j) = DI_{j1} + CI_{j2} = DI_{j1} + C\left\{\frac{1}{2}\ln \mathrm{X} - AI_{j1}\right\}$$

$$J_j = (D - AC)I_{j1} + \frac{C}{2}\ln \mathrm{X} = \frac{D - AC}{E}\left\{\tan^{-1}\frac{l_j + A}{E} - \tan^{-1}\frac{A}{E}\right\} + \frac{C}{2}\ln\frac{l_j^2 + 2Al_j + B}{B}$$

$$D - AC = (x_i - x_{j0})\cos\delta_i + (z_i - z_{j0})\sin\delta_i$$

$$-[-(x_i - x_{j0})\cos\delta_i - (z_i - z_{j0})\sin\delta_i](-\cos(\delta_j - \delta_i))$$

$$[(x_i - x_{j0})\cos\delta_i + (z_i - z_{j0})\sin\delta_i](-\sin\delta_i \sin\delta_j - \cos\delta_i \cos\delta_j)$$

$$= (x_i - x_{j0})[\cos\delta_i - \sin\delta_i \sin\delta_j \cos\delta_j - \cos\delta_i \cos^2\delta_i]$$

$$(z_i - z_{j0})[\sin\delta_i - \sin\delta_i \sin^2\delta_j - \cos\delta_i \cos\delta_j \sin\delta_j]$$

$$= (x_i - x_{j0})[\cos\delta_i(1 - \cos^2\delta_j) - \sin\delta_i \sin\delta_j \cos\delta_j]$$

$$(z_i - z_{j0})[\sin\delta_i(1 - \sin^2\delta_j) - \cos\delta_i \cos\delta_j \sin\delta_j]$$

$$= (x_i - x_{j0})\sin\delta_j[\cos\delta_i \sin\delta_j - \sin\delta_i \cos\delta_j] - (z_i - z_{j0})\cos\delta_j[-\sin\delta_i \cos\delta_j + \cos\delta_i \sin\delta_j]$$

where $\frac{D - AC}{E} = -\sin(\delta_i - \delta_j)$

53

A Class of Airfoils Designed for High Lift in Incompressible Flow

Robert H. Liebeck*
Douglas Aircraft Company, McDonnell Douglas Corporation, Long Beach, Calif.

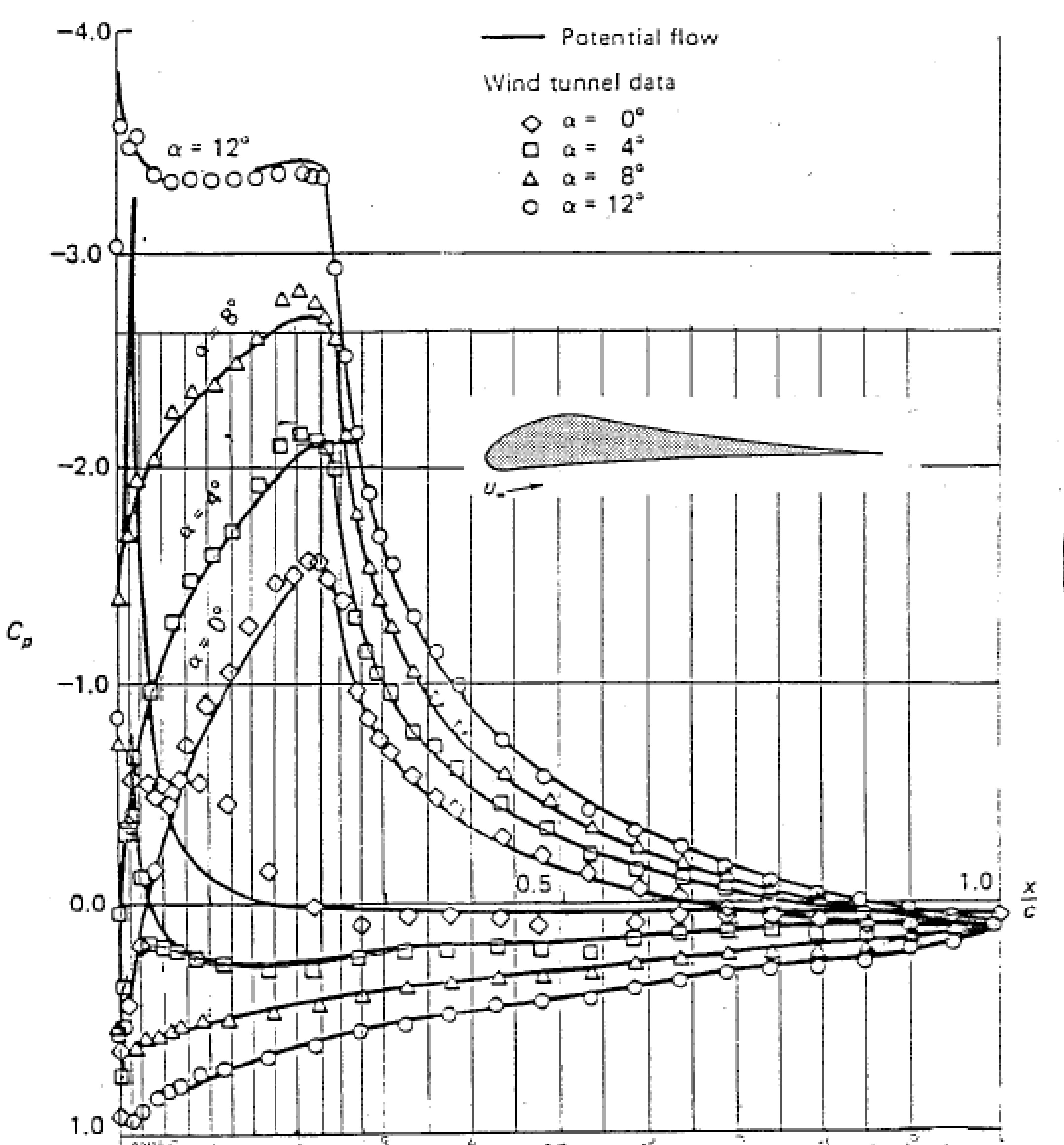

FIGURE 4-15 *A comparison of the theoretical potential-flow and the experimental pressure distribution for a high-lift, single-element airfoil, $Re_c = 3 \times 10^6$ (from Ref. 4.6).*

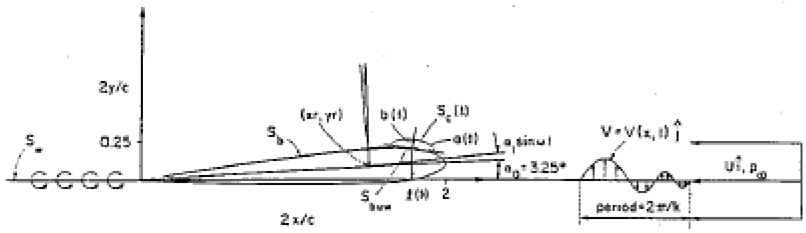

Figure 1. Cavity and foil geometry.

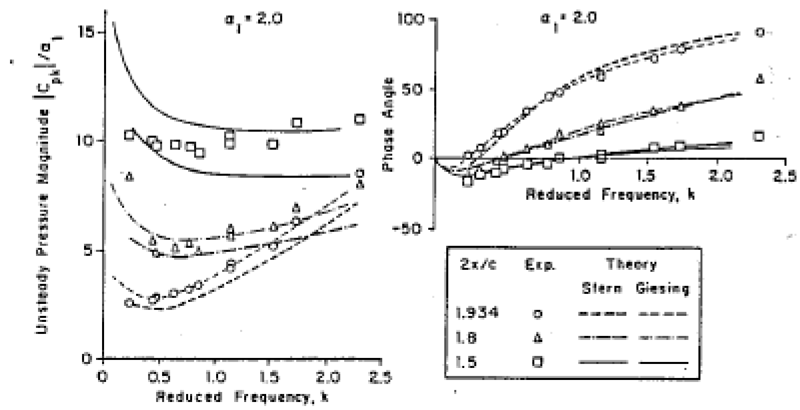

Figure 2. Noncavitating flow unsteady pressure magnitude and phase angle.

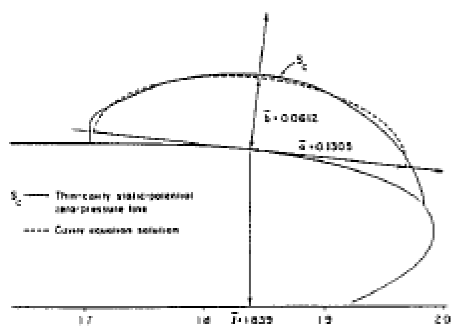

Figure 3. Steady-cavity solution: $\alpha_0 = 4.3^o$.

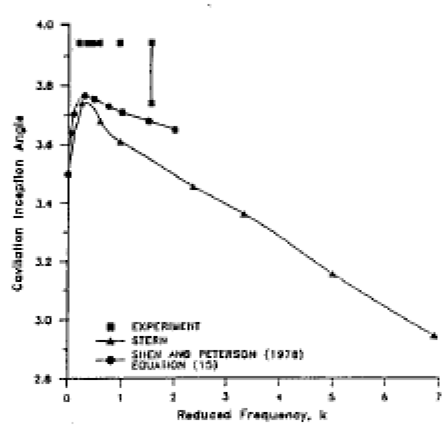

Figure 4. Cavitation inception angles: $\alpha_1 = .95^o$.

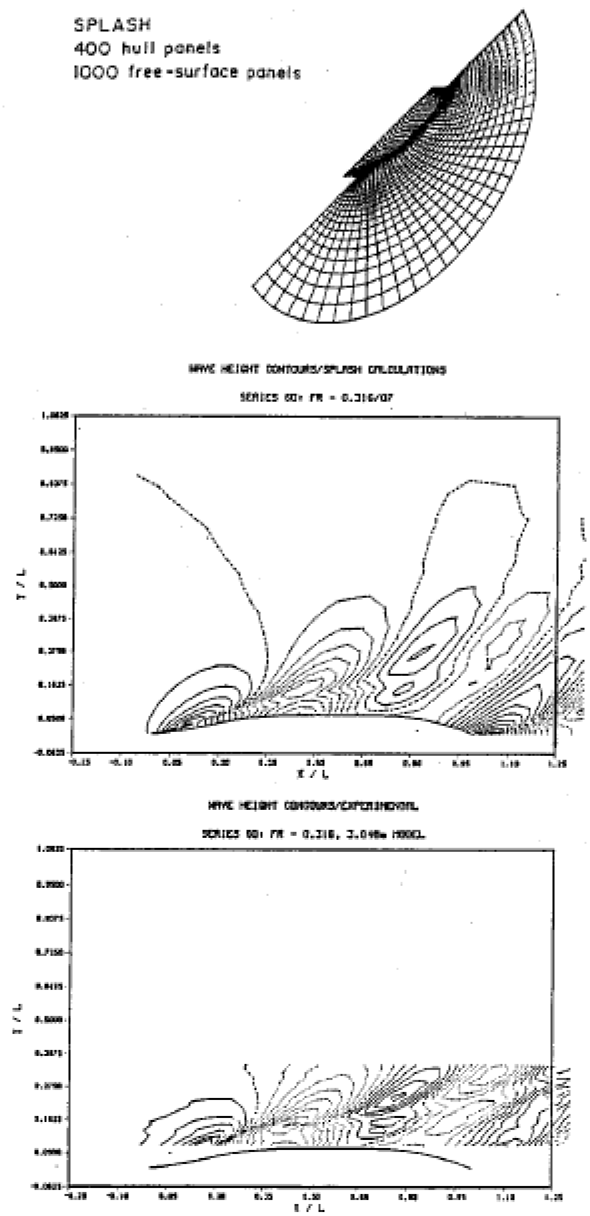

Figure 10. SPLASH hull and free-surface panels and SPLASH and experimental wave-height contours.

56

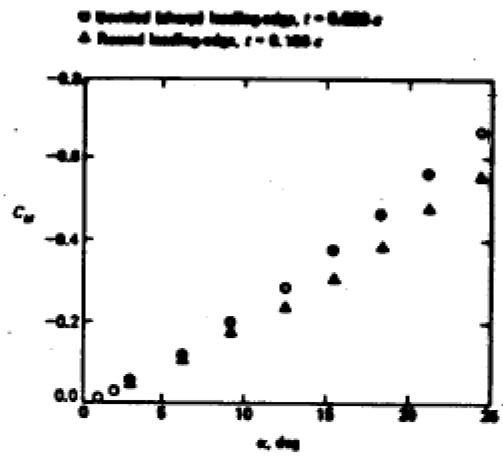

FIGURE 6-38 *The moment coefficient (about the apex) for thin, flat delta wings for which AR = 1.5, Re_c = 6 × 10⁴ (data from Ref. 6.19).*

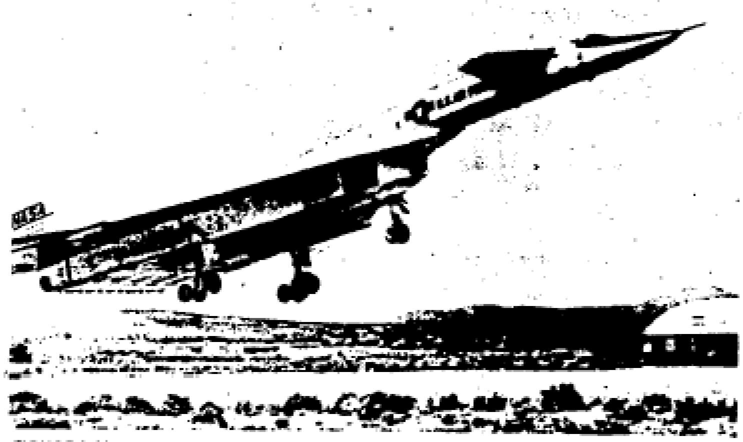

FIGURE 6-39 *Photograph of the North American XB-70 illustrating the use of canards (Courtesy, NASA).*

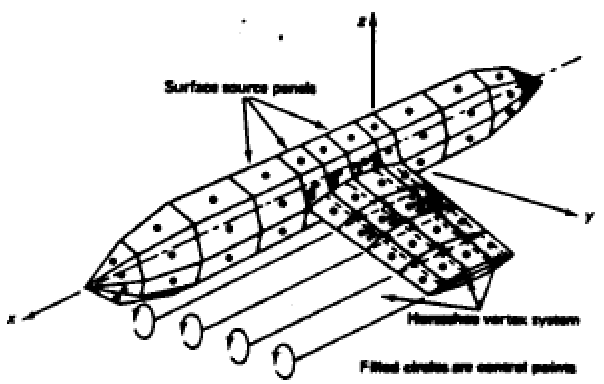

FIGURE 6-40 *Source and vortex lattice-panel arrangement for a wing/body configuration for zero yaw, i.e., xz plane is a plane of symmetry.*

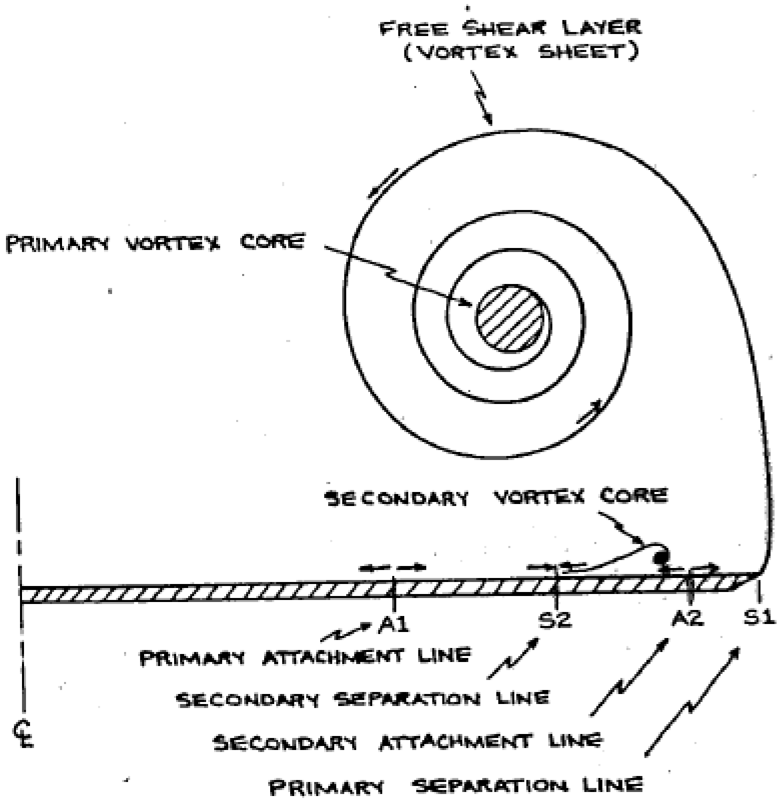

Figure 4.1.6 - Flow pattern in crossflow plane on delta wing'

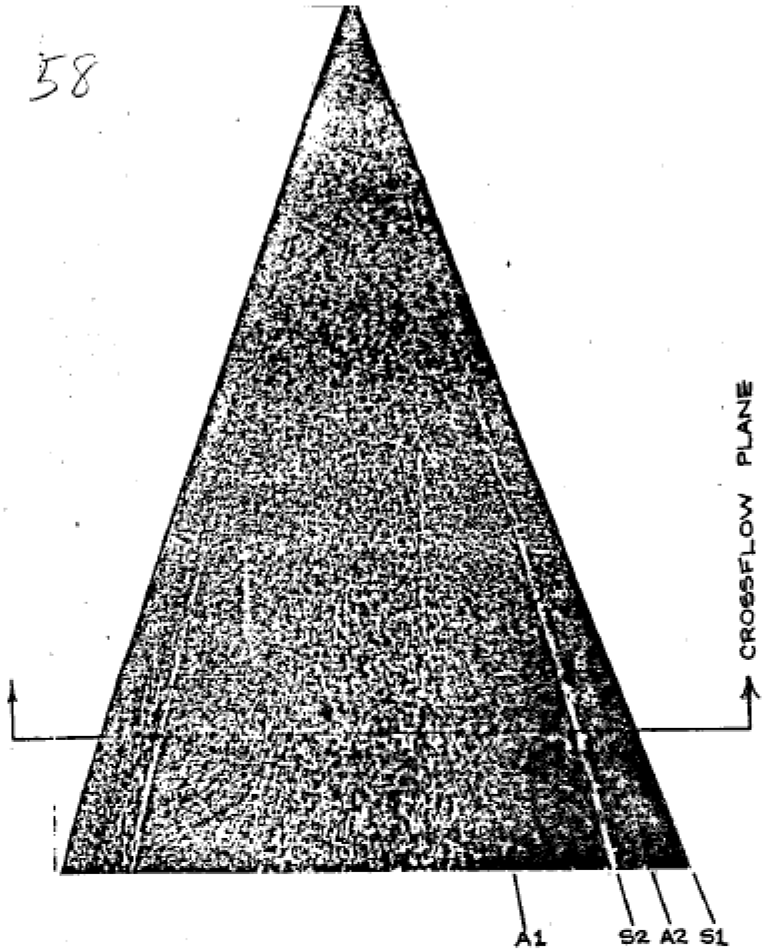

(From Marsden, Simpson, and Rainbird, 1958)

Figure 4.1.5 - Surface flow visualization on upper surface of delta wing ($\alpha = 14°$)

59

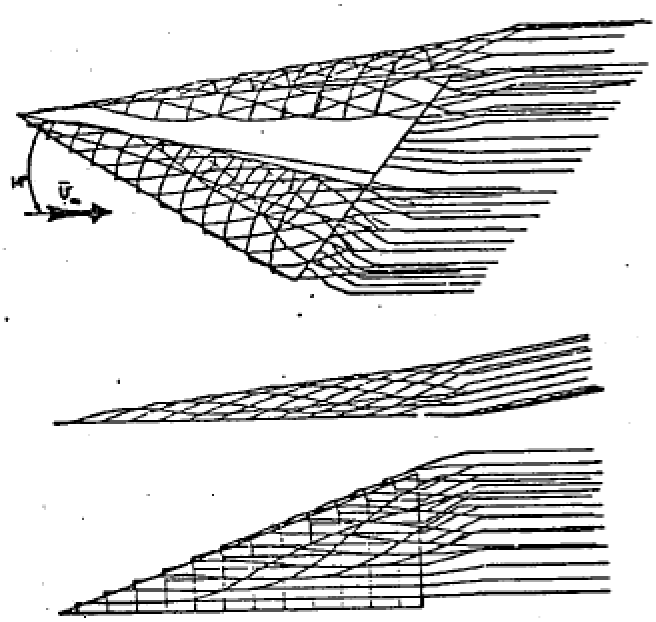

(From Kandil, Mook, & Nayfeh, 1976)

Figure 5.2.2 - Typical solution of wake shape for a delta wing using Kandil, Mook, & Nayfeh model

60

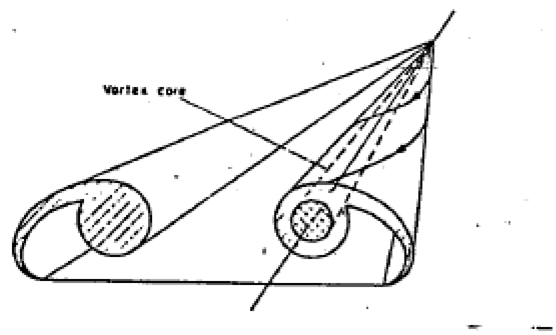

(From Hall, 1966)

Figure 4.1.3 – Vortex cores over slender delta wing

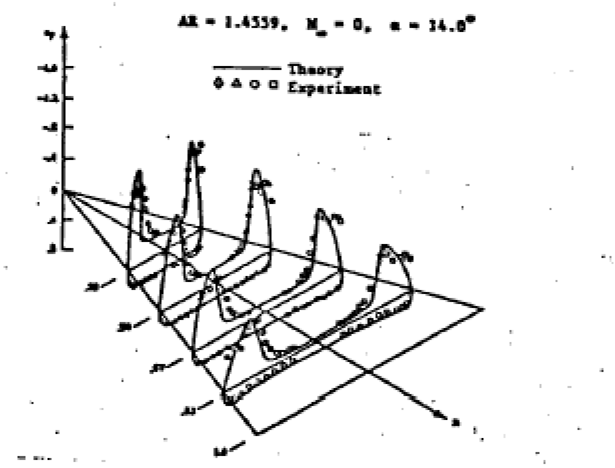

(From Smith, 1978)

Figure 4.1.4 – Pressure distribution on upper surface of delta wing

61

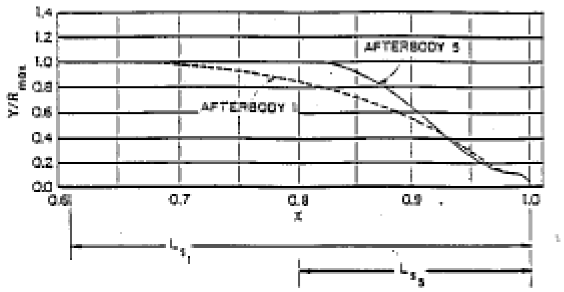

Figure 21. Geometric Data for DTNSRDC Afterbodies 1 and 5

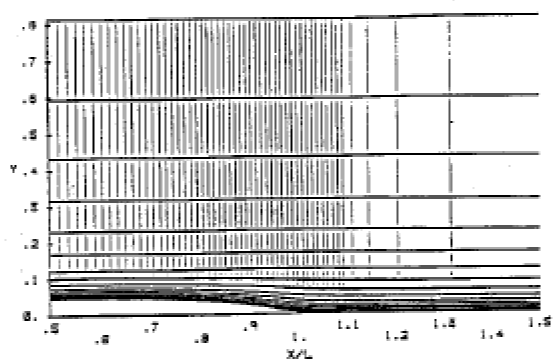

Figure 22. Large-Domain Grid for Afterbody 1

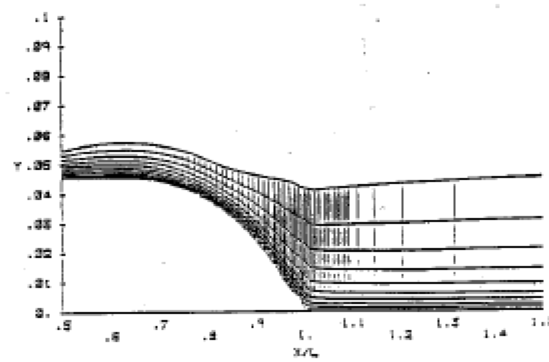

Figure 23. Small-Domain Grid for Afterbody 1

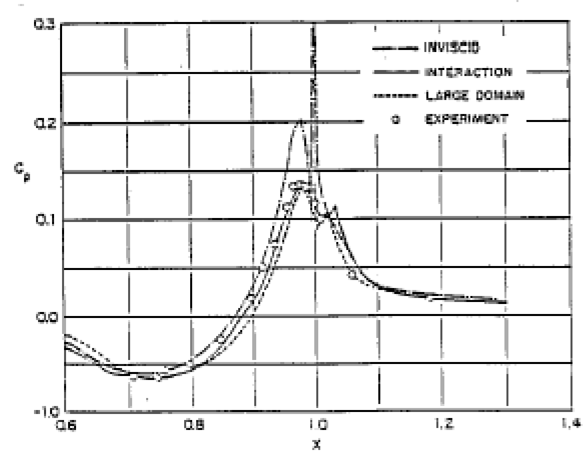

Figure 24. Pressure Distribution on the Surface of the Body and along the Wake Centerline